Numerical Study on Filtration of Soot Particulates in Gasoline Exhaust Gas by SiC Fiber Filter

Kazuhiro Yamamoto[1,a] and Yusuke Toda[1,b]

[1]Nagoya University, Department of Mechanical Science and Engineering, Furo-cho, Nagoya-shi, Aichi 464-8603, Japan

[a] kazuhiro@mech.nagoya-u.ac.jp, [b] toda@eess.mech.nagoya-u.ac.jp

Keywords: Filtration, Nanoparticles, SiC fiber, Gasoline particulate, Numerical simulation.

Abstract. As for gasoline vehicles, the particulate matter (PM) emissions from traditional port fuel injection (PFI) engines are pretty low. Recently, the gasoline direct injection (GDI) vehicles have been gaining market share globally due to better fuel efficiency, especially in the European countries. A drawback associated with GDI engines is considerably higher PM emissions compared with PFI engines. The soot in gasoline exhaust gas would contribute to urban air pollution, which is deeply related with adverse health effects. For the reduction of PM emission in Europe, a new regulation known as EURO VI has been set recently. Then, we need to trap soot particles in exhaust gas from gasoline automobiles as well as diesel automobiles. However, the gasoline soot would be much smaller than the diesel soot. Also, the gasoline exhaust gas temperature is much higher. Then, we need gasoline particulate filter (GPF) which needs to have better thermal durability. In this study, as a potential GPF, an SiC fiber filter was numerically examined. The effect of the fiber diameter on the filtration was revealed. Results show that, when the filter of the larger fiber diameter is placed more upstream, the deposition of soot particles widely occurs inside the filter, resulting in the lower pressure drop.

Introduction

The soot emission from internal combustion engines would contribute to urban air pollution, which is deeply related with adverse health effects [1]. It has long been considered as one of the major sources of anthropogenically generated particulate matters (PM), stimulating regulatory authorities worldwide to introduce continuously tighter emission standards [2]. Thus, a well-known diesel particulate filter (DPF) is needed in most diesel vehicles for the exhaust after-treatment [3].

As for the gasoline vehicles, the situation is rather complicated, because PM emissions from the traditional port fuel injection (PFI) engines are pretty low. Recently, the gasoline direct injection (GDI) vehicles have been gaining market share globally due to better fuel efficiency, especially in the European countries [4]. A drawback associated with GDI engines is considerably higher PM emissions compared with PFI engines. For the reduction of particulate emission in Europe, a new regulation known as EURO VI has been set recently. Then, we also need to trap soot particles in gasoline exhaust gas by a gasoline particulate filter (GPF). Unfortunately, the deposited particles inside the filter could be a barrier or block for the flow, and the unexpected pressure rise may worsen the fuel consumption rate. It should be noted that gasoline particulates would be much smaller than diesel particulates [2]. Also, the gasoline exhaust gas temperature is much higher. Thus, in order to provide sufficient particle reduction, an establishment of a new filtration system by using materials with enough thermal durability as well as the lower filter backpressure would be urgently required.

In the present study, as a potential non-catalytic system, we focused on the material of SiC fibers. In our previous study, we have tested the filtration system with SiC fiber by an engine test bench [5]. Since the porosity of SiC fiber is over 0.9, the filter backpressure is expectedly low. Another advantage of SiC fiber is that the thermal durability of fiber is enough up to 1800 ℃. It is one of the advanced materials, so that any catalysts for the oxidation of exhaust particles are not needed. One difficulty is that we cannot directly observe the phenomena inside the filter. The numerical simulation

is the only way to reveal the process of PM trap. Then, for discussing the soot deposition region, which cannot be observed in experiments, we simulated the filtration process by the SiC fiber.

Numerical Model

Lattice Boltzmann Method. Here, our numerical model is explained. The numerical scheme of a lattice Boltzmann method, or simply LBM, is well-known to be suitable for the fluid simulation in porous media. The variable for describing the flow is the distribution function of the particles, composed of the streaming process of fluids to next lattice during one time setup, and the collision process relaxed to the equilibrium by particles' collision. To reproduce the flow in the real filter, a three-dimensional simulation was performed. The 3D 15-velocity model (called d3q15) was used to discrete the time and the space in the numerical domain. To discuss the pressure rise during the filtration process, the flow passing through the deposited soot layer must be taken into consideration. In the equation of the LBM, we considered the external force term [6]. Then, the local equilibrium distribution functions are expressed by the following equations (1) and (2):

$$f_{p,i}(\boldsymbol{x}+\boldsymbol{e}_i\delta_t, t+\delta_t) - f_{p,i}(\boldsymbol{x},t) = -\frac{1}{\tau_p}[f_{p,i}(\boldsymbol{x},t) - f_{p,i}^{eq}(\boldsymbol{x},t)] - \frac{\tau_p - 0.5}{\tau_p}F_i \tag{1}$$

$$f_{p,i}^{(eq)} = w_i\left\{p + p_0\left[3\left(\frac{\boldsymbol{e}_i\cdot\boldsymbol{u}}{c^2}\right) + \frac{9}{2}\left(\frac{\boldsymbol{e}_i\cdot\boldsymbol{u}}{c^2}\right)^2 - \frac{3}{2}\left(\frac{\boldsymbol{u}}{c}\right)^2\right]\right\} \tag{2}$$

Here, w_i = 1/9 (i = 1−6), 1/72 (i = 7−14), and 2/9 (i = 15), $c = \delta_x/\delta_t$, where δ_x and δ_t represent the grid size and time step. The variable of p_0 represents the pressure of the atmosphere. The relaxation time τ_p in Eq. (1) is related with the kinematic viscosity, ν, characterized by

$$\nu = \frac{2\tau_p - 1}{6}\frac{\delta_x^2}{\delta_t} \tag{3}$$

The total pressure of p, the velocity of $\boldsymbol{u}$, the external force of $\boldsymbol{f}$ and the external force term F_i are expressed by the following equations.

$$p = \sum_i f_{p,i} \tag{4}$$

$$\boldsymbol{u} = \sum_i \boldsymbol{e}_i f_{p,i} / p_0 + 0.5\boldsymbol{f}\delta_t \tag{5}$$

$$\boldsymbol{f} = -\frac{\nu}{\kappa}\boldsymbol{u} \tag{6}$$

$$F_i = \frac{-3\boldsymbol{f}\cdot(\boldsymbol{e}_i - \boldsymbol{u})}{c^2} f_{p,i}^{(eq)} \tag{7}$$

The variable of κ in Eq. (6) is the permeability of soot layer. By considering the fact that the soot layer has many pores, there is the flow passing through the soot layer. Then, the permeability of the soot region (sometimes called soot cake) is modelled to fit the value in the real exhaust gas flow. It is reported that when the exhaust gas temperature is 573 K, the typical value of the soot layer permeability is 2.0×10^{-14} m^2 [7], which was used in the simulation.

To describe the concentration of soot in exhaust gas, the soot concentration in the gas phase must be described. Then, in addition to the distribution function of the pressure, that of soot concentration is also needed, which is expressed by the equations of (8) and (9).

$$f_{c,i}(\mathbf{x}+\mathbf{e}_i\delta_t, t+\delta_t) - f_{c,i}(\mathbf{x},t) = -\frac{1}{\tau_c}[f_{c,i}(\mathbf{x},t) - f_{c,i}^{(eq)}(\mathbf{x},t)] \tag{8}$$

$$f_{c,i}^{(eq)} = w_i Y_c \left\{ 1 + 3\left(\frac{\mathbf{e}_i \cdot \mathbf{u}}{c^2} \right) + \frac{9}{2}\left(\frac{\mathbf{e}_i \cdot \mathbf{u}}{c^2} \right)^2 - \frac{3}{2}\left(\frac{\mathbf{u}}{c} \right)^2 \right\} \tag{9}$$

The soot concentration, corresponding to the soot mass fraction, is obtained by

$$Y_c = \sum_i f_{c,i} \tag{10}$$

In Eq. (8), the relaxation time of τ_c is set to be the same value of τ_p in Eq. (1).

Soot Deposition Model. Due to the computational costs, it must be impractical to consider the real structure of the gasoline soot, because the soot is carbonaceous agglomerates with primary particles [7]. To avoid this, our model only includes the soot mass fraction in both the gas phase, not the real geometry of the gasoline soot, by which the formation of the deposited soot layer is realized. Uniquely, the soot deposition probability on the fiber filter of P_D was determined experimentally [8], and the value of 0.001 was used.

The procedure of the soot deposition process is explained in Fig. 1. At one time step of IT_1, the soot arrives around the filter substrate, corresponding to one lattice node in the Fig. 1a. Since the value of P_D is the model parameter, and only the fraction of P_D is deposited. That means, the fraction of (1－P_D) is not trapped on the filter surface, and is transported by the original gas flow. Continuously, the total soot arriving at the lattice point is increased. At some time, the mass fraction of soot becomes unity at the time step, IT_2. Then, this node is treated as the solid phase of the soot layer, instead of the gas phase. At the time step of IT_2 + 1, the node for the soot deposition is shifted to the next node (grid point). In this manner, the layer of the soot region is thickened in the process of the soot layer growth.

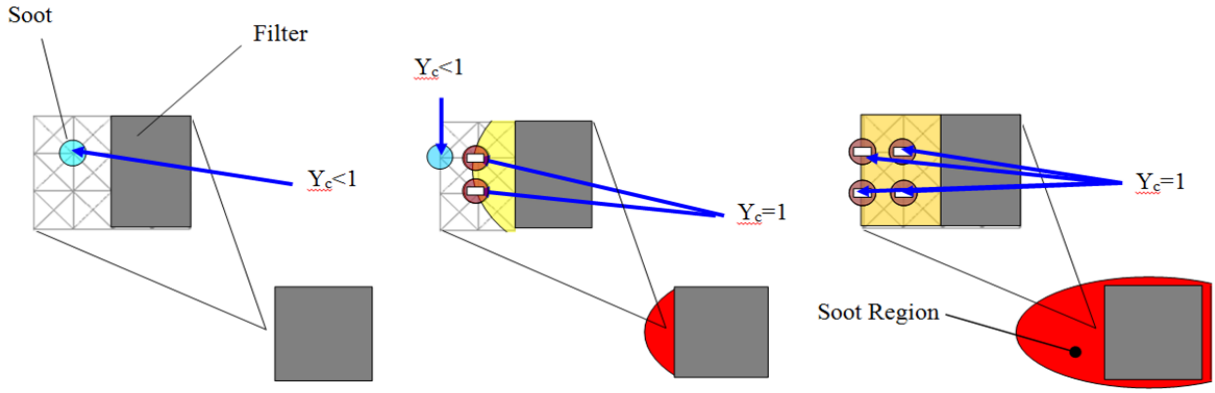

(a) time step of IT_1 (b) time step of IT_2 (c) time step of IT_2 + 1

Fig. 1. Soot deposition model.

Numerical Domain. The numerical domain and the coordinate are shown in Fig. 2. To model the fiber structure (see Fig. 3a), the straight fiber rods of the constant diameter were randomly placed in the filter region with fixed porosity of 0.9, which is shown by the dotted box. The filter region is 250 μm (x) × 125 μm (y) × 125 μm (z), and x is the inflow direction. The total calculation domain is 375 μm (x) × 125 μm (y) × 125 μm (z), with grids of 151 (N_x) × 51 (N_y) × 51 (N_z). The grid size is 2.5 μm.

For the boundary condition, the inflow boundary was adopted at the inlet. The velocity at the inlet (the inflow velocity) was 10 cm/s, which was the same value in experiments. Since we simulated the filtration of soot particles in cold flow, the inlet gas temperature was 25 ℃. The mass fraction of soot particles was 4.54×10^{-5} [9]. At four side walls, the slip boundary condition was set, assuming the symmetry. At the filter outlet, the pressure was constant. The gradient of soot mass fraction was set to be zero. On the filter surface, the non-slip boundary condition was adopted.

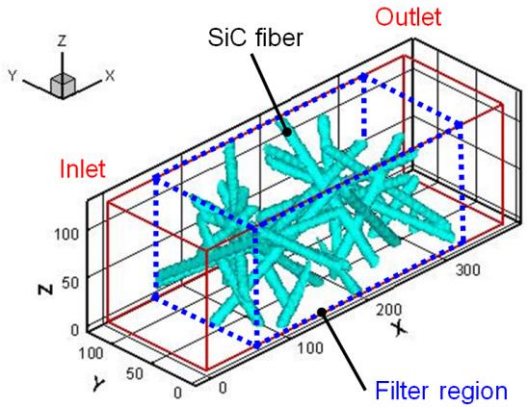

Fig. 2. Coordinate and calculation region are shown. SiC fibers are randomly set in filter region shown by dotted box.

Results and Discussion

Observation of Fiber with Trapper Particles. First, the filtration of the soot trap by the SiC fiber is explained. To visualize the deposition region of the soot layer, images of 0 min (before deposition), 30 min, and 90 min of filtration time, *t*, are shown in Fig. 3, which were obtained by a laser beam microscope (VK-9500; Keyence Corporation, Japan). The fiber diameter is 10 μm. As seen in Fig. 3a, its structure is nearly the assembly of straight-line fibers. The soot particles are deposited along the fibers in Fig. 3b, whereas the dense layer of soot particles is formed in Fig. 3c.

As for the fiber filtration, three mechanisms are proposed [10]: surface straining, depth filtration, and cake filtration. In the surface straining, only the large particles are trapped, yet smaller particles pass through. Since the size of soot particles is much smaller than fiber spacing, the surface straining may seldom occur. In the depth filtration, the particle attaches to the fiber by inertial impaction, direct interception, Brownian deposition, electrostatic attraction and gravity settling, apparently corresponding to Fig. 3b. In the cake filtration corresponding to Fig. 3c, once the full layer of the soot on the filter surface is formed, which is called a soot cake layer, the filtration efficiency becomes 100 % [6]. Thus, similar to the diesel soot, the well-known transition from the depth filtration to the surface filtration [6] was observed in the filtration process of SiC fibers.

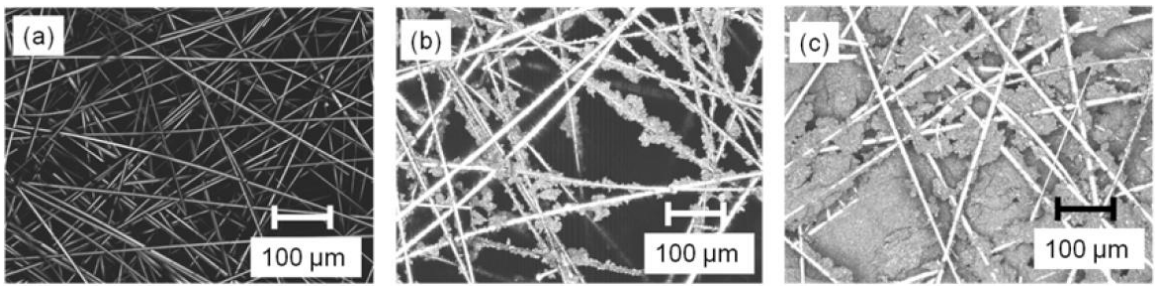

Fig. 3. Laser microscope images of SiC fibers with trapped particles; (a) t = 0 min (b) 30 min (c) 90 min.

Filtration in Simulation. Here, effects of fiber diameter were examined. Two fiber diameters of 10 and 14 μm were considered. To improve the filtration efficiency without the penalty of higher pressure drop (filter backpressure), the combination of several filter sheets of different fiber diameter was tested. To set the filter of different fiber diameter, the filter region shown by the dotted box in Fig. 2 was divided into two areas of upstream and downstream sections to set a pair of sheets. Three cases were considered: two 10 μm-diameter sheets, two 14 μm-diameter sheets, and the combination of 14-10 μm-diameter sheets. For three cases, the porosity of the filter region was the constant value of 0.9. Each sheet thickness in the simulation was 125 μm. Fig. 4 shows 3D profiles of soot deposition region in two 10 μm-diameter sheets. The filtration time of *t* was 1.3, 7.5, or 13.8 s. The light blue

region is the SiC fiber, and the black region is the deposition region of soot particles. It is observed the SiC fiber is gradually covered with soot particles during the filtration.

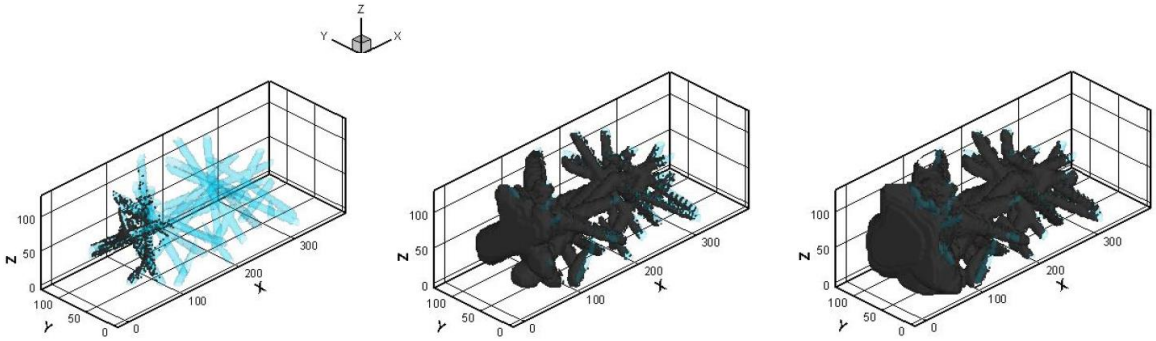

(a) (b) (c)

Fig. 4. Soot deposition region in at (a) t = 1.3 s, (b) t = 7.5 s, and (c) t = 13.8 s.

Fig. 5 shows the distribution of mass of soot particles along the flow direction of x. The averaged value in y-z plane at t = 13.8 s is shown. Results of two 10 μm-diameter sheets, two 14 μm-diameter sheets, and the combination of 14-10 μm-diameter sheets are compared. It is seen that more soot particles are deposited at the upstream section of 62.5 μm < x < 187.5 μm. The leakage of soot particles through the upstream section are trapped at the downstream section of 187.5 μm < x < 312.5 μm. At the upstream section, the 10 μm-diameter sheet shows the better filtration. It is emphasized that, in case of 14-10 μm-diameter sheets, more soot particles are trapped at the downstream section. It is worth noting that the deposition of soot particles widely occurs in 14-10 μm-diameter sheets.

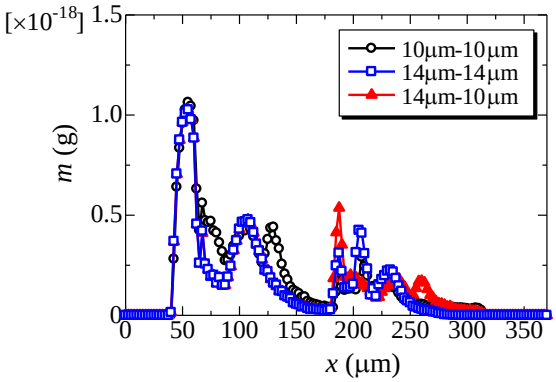

Fig. 5. Distribution of soot mass at t = 13.8 s.

Fig. 6 shows the time-variation of filtration efficiency and the pressure drop, compared between three cases. The filtration efficiency (f_m) by Eq. (11) is based on the soot mass:

$$f_m = \frac{\iint_{in} \rho Y_c dydz - \iint_{out} \rho Y_c dydz}{\iint_{in} \rho Y_c dydz} \tag{11}$$

where ρ is the true density of soot particles, Y_c is the soot mass fraction, and the subscript of "in" or "out" is the value at the filter inlet or outlet. The filtration of two 10 μm-diameter or 14-10 μm-diameter sheets is better, whereas that of two 14 μm-diameter sheets is the worst. On the other hand, the pressure drop of two 10 μm-diameter sheets is much higher than other two cases. Expectedly, as more soot is deposited, the pressure drop increases. However, in Fig. 6, the pressure drop of 14-10 μm-diameter sheets almost matches that of two 14 μm-diameter sheets. This could be explained by the fact that the pressure drop depends on where the deposition of soot particles occurs. Therefore, the combination of 14-10 μm-diameter sheets could be the best. It is concluded that, when

the filter of the larger fiber diameter is placed more upstream, the deposition of soot particles would widely occur inside the filter, resulting in the lower pressure drop.

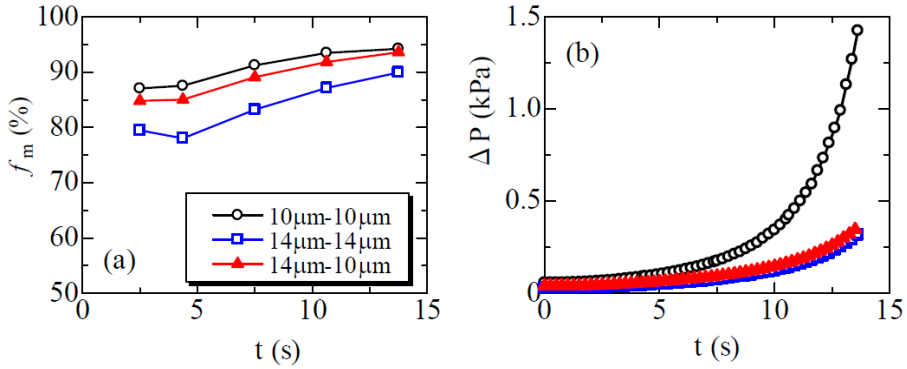

Fig. 6. Time-variation of (a) filtration efficiency and (b) pressure drop at different fiber diameter.

Summary

In this study, as a potential of gasoline particulate filter (GPF), the SiC fiber filter was tested. We conducted the numerical simulation of the soot filtration, focused on the fiber diameter. As the fiber diameter is smaller at the constant porosity, the filtration efficiency becomes higher. The combination of 14-10 μm-diameter sheets placed from the upstream in this order shows the better filtration and the lower pressure drop. It is confirmed that, when the filter of the larger fiber diameter is placed more upstream, the deposition of soot particles widely occurs inside the filter, resulting in the lower pressure drop.

More experimental works will be done for optimizing the combination of the fiber diameter to trap particles efficiently, collaborated with the engine test bench already similarly applied to the real diesel particulate filters [5, 11, 12].

References

[1] I.M. Kennedy, Proc. Combust. Inst. 31, 2757 (2007).

[2] A. Mamakos, G. Martini, A. Marotta, U. Manfredim, J. Aerosol Sci. 63, 115 (2013).

[3] T.V. Johnson, SAE Technical Paper 2010-01-0301, 16 (2010).

[4] S. Spiess, K.-F. Wong, J.-M. Richter, R. Klingmann, Top Catal. Vol. 56, 434 (2013).

[5] K. Yamamoto, F. Fujikake, K. Matsui, Proc. Combust. Inst. Vol. 34, 2865 (2013).

[6] K. Yamamoto, S. Ohori, Int. J. Engine Research 14, 333 (2013).

[7] A.G. Konstandopoulos, E. Skaperdas, SAE Technical Paper 2002-01-1015, 1 (2002).

[8] K. Yamamoto, K. Yamauchi, N. Takada, M. Misawa, H. Furutani, O. Shinozaki, Philosophical Transaction A, 369, 2584 (2011).

[9] K. Yamamoto and K. Yamauchi, Proc. Combust. Inst. 34, 3083 (2013).

[10] R.S. Barhate, S. Sundarrajan, D. Pliszka, S. Ramakrishna, Filtration & Separation, 45, 32 (2008).

[11] K. Tsuneyoshi, and K. Yamamoto, Energy, 48, 492 (2012).

[12] K. Tsuneyoshi, and K. Yamamoto, Energy, 60, 325 (2013).